Journal of Power Sources 202 (2012) 184–189

Contents lists available at SciVerse ScienceDirect

Journal of Power Sources

journal homepage: www.elsevier.com/locate/jpowsour

Durability of carbon–silica supported catalysts for proton exchange membrane fuel cells

F. Dundar[a,c,*], A. Uzunoglu[a], A. Ata[a], K.J. Wynne[b]

[a] Nanotechnology Research Center, Gebze Institute of Technology, 41420 Kocaeli, Turkey
[b] Department of Chemical and Life Science Engineering Dept., Virginia Commonwealth University, Richmond, VA 23284-3028, United States
[c] Department of Mechanical Engineering, Meliksah University, 38280, Kayseri, Turkey

ARTICLE INFO

Article history:
Received 17 August 2011
Received in revised form 11 October 2011
Accepted 6 December 2011
Available online 16 December 2011

Keywords:
Proton exchange membrane fuel cells
Catalyst
Durability
Carbon–silica
Aerogel
Accelerated test

ABSTRACT

Carbon-aerogel silica composite material is evaluated as an alternative catalyst support material for Proton Exchange Membrane (PEM) fuel cells. Brunauer–Emmett–Teller surface areas of these materials are usually higher than Vulcan XC-72 which enabled a homogeneous catalyst distribution. Performance of the Membrane Electrode Assemblies (MEAs) prepared with C-SiO_2 supported platinum catalysts increased with low silica content and decreased at higher levels. Performances up to 0.31 W cm^{-2} at 0.8 V are obtained with silica containing MEAs whereas only 0.23 W cm^{-2} at 0.8 V could be obtained with silica free MEAs. On the other hand, durability of the MEAs increased with increasing silica content. Accelerated durability tests show a current drop of 22–40% (at 0.6 V) for silica containing MEAs compared to 40% (at 0.6 V) for silica-free MEAs. Although appearing to have improved durability, silica containing MEAs show hydrophilic behavior, especially at high current density.

1. Introduction

Spurred by the need for alternate energy sources, proton exchange membrane (PEM) fuel cell systems have been developed and commercialized. "Durability" is a term that covers many problems encountered in these systems. PEM fuel cell failure may be initiated by membranes loosing conductivity, [1] undergoing crystallization [2] or by chemical or mechanical degradation [3–8]. Catalyst layers may experience poisoning, dissolution, agglomeration or corrosion of platinum, support material or ionomer matrix [9]. Gas diffusion layers can lose hydrophobicity, porosity or low contact resistance [9,10]. Bipolar plates can corrode or lose low contact resistance [11,12] and gaskets can corrode, dissolve or loose impermeability [13,14]. Additionally, oxidation of contact points or separation of layers can be counted as durability problems [15]. Catalyst layer degradation is certainly a critical problem among other durability issues since the catalyst, typically Pt, is an expensive component of a fuel cell system [16]. Carbon supported platinum catalysts are commonly used fuel cell catalysts both for anode and cathode reactions. These catalysts have acceptable durability at ideal fuel cell operating conditions. However, combinations of unfavorable conditions, such as both high potentials and high liquid water content, results in premature catalyst degradation [17]. Other high stress conditions include limited fuel feed at startup, limited oxidant feed, flooding and channel blockage, and low limiting current density at the anode. These circumstances may result in high potentials either at the anode or cathode with concomitant catalyst degradation [18].

The most common degradation mechanisms for PEM fuel cell catalyst layers are platinum agglomeration, platinum dissolution, platinum poisoning and carbon corrosion [9]. All of these processes result in decreased fuel cell performance. While some of these processes are reversible [9,19] in most cases the catalyst layer becomes nonfunctional [20].

Carbon based materials are commonly used as catalyst support materials due to their high surface area, corrosion resistance under ideal fuel cell operating conditions and acceptable conductivity. Alternative forms of carbon that may improve performance and durability are under investigation. Carbon nanotubes [21–26], conductive ceramics [27], carbon-polymer composites [28], mesoporous carbons [29,30], graphitized carbons [31,32], nitrided graphitized carbons [33], carbides [34–36], whisker like structures [37] and carbon aerogels [38] are promising candidate materials as alternatives to often used Vulcan XC-72.

The conductivity of carbon and durability of silica have been combined by synthesizing nanocomposites. A number of methods have been used to introduce a second component such as

* Corresponding author at: Mechanical Engineering Dept., Meliksah University, 38280 Kayseri, Turkey. Tel.: +90 533 578 9251; fax: +90 352 207 7349.
E-mail address: fdundar@meliksah.edu.tr (F. Dundar).

0378-7753/$ – see front matter © 2011 Elsevier B.V. All rights reserved.
doi:10.1016/j.jpowsour.2011.12.010

carbon into the siliceous phase [39]. As the colloidal silica gels form through condensation polymerization, the second phase is incorporated. Second phase incorporation was used for continuous mesoporous structure generation [40], reduced thermal conductivity [41], reduced aggregation [42], improved thermal stability [43], obtaining crack-free transparent films [44] or uniform dispersion of the active material [45].

Carbon-aerogel silica catalyst support for fuel cell concept was studied by several researchers. Morris et al. used aerogel silica as a nanoglue to prevent carbon support agglomeration [46]. Anderson et al. stated that heterocyclic sulfur present in the structure of Vulcan XC-72 was bound to silica particles rather than poisoning platinum particles [40]. Takenaka et al. coated the surface of carbon nanotubes with an extremely thin silica layer and reported improved durability [47]. Previous work from our laboratory showed superior thermal stability and improved performance of Pt on carbon modified by relatively small amounts of a sol–gel generated siliceous component [48]. Below, we report an extension of this work that suggests silica modified carbon supported Pt has improved durability compared to carbon supported Pt.

2. Experimental

2.1. Pt/C-SiO_2 catalyst preparation

Vulcan XC-72 was kept in a vacuum oven at 200 °C in order to clean the surface. Methanol (36 ml) and water (24 ml) were added to 1 g cleaned Vulcan XC-72. The mixture was homogenized with Hielscher 400S ultrasonic homogenizer for 5 min. Desired C-SiO_2 concentrations were achieved by adding Tetramethyl ortho silicate (TMOS) to the mixture. Additional deionized water (40 ml) was added for effective hydrolysis of siliceous components during the 96 h stirring process. The mixture was filtered and washed with methanol-water solution three times. The cake was dried in a vacuum oven at 60 °C and then ground with an agate mortar and pestle and sieved with a 60 mesh grid. A nearly full conversion to SiO_2 is obtained by heating at ≤100 °C [48]. For brevity, the $SiO_2 \cdot H_2O$ product will be simply designated as silica.

Carbon or carbon–silica supported Pt catalysts were synthesized by the $NaBH_4$ reduction method [49]. Water (14 ml) was added to 5.6 mg $NaBH_4$ and the solution was cooled down to 0 °C. An 8–10 times $NaBH_4$ excess was chosen for rapid Pt nanoparticle generation. Meanwhile, 4 ml methanol and 6 ml water were added to 50 mg support carbon and the mixture was homogenized with an ultrasonic homogenizer at 0 °C for 5 min with intermittent full power. The cold $NaBH_4$ solution was poured into the support material mixture and the combination was homogenized for 1 min at full power. After homogenization, the support mixture was rapidly poured into vigorously stirred 1.3 mM $H_2PtCl_6 \cdot 6H_2O$ solution.

2.2. Composition analysis with TGA

TGA was used to determine support and catalyst compositions by monitoring mass change due to carbon combustion. Specimens (3–5 mg) were dried in a vacuum oven before analysis. The heating rate was 10 °C min^{-1} with air as the carrier gas. Support materials were heated to 800 °C whereas catalysts were heated to 650 °C.

2.3. Surface area measurements with BET

N_2 Bruanuer–Emmett–Teller (BET) surface areas of the prepared support materials were determined using Autosorb 1B surface area analyzer (Quantachrome Inc.) [50]. Trapped gas was removed with overnight heating under vacuum at 300 °C. Specimen weights were calculated immediately after the degassing process. Minimum and maximum P/P_0 values were selected as 0.05–0.3 to observe the "knee" formation clearly as suggested by the manufacturer. P/P_0 increments were selected logarithmically. Data points, covering only the "knee" zone, were selected for Multipoint BET surface area calculations.

2.4. Particle size determination with DLS

Support material particle size distributions were determined with using Zetasizer Nano ZS (Malvern Instruments). Support materials were dispersed in water right before the analysis using Hielsher 400S ultrasonic homogenizer at full power for 30 s. Average of 9 measurements were recorded to collect a data point and 5 repeat experiments were carried out for all specimens.

2.5. MEA preparation

A screen printing method coupled with decal transfer process was selected for the MEA preparation [51]. Catalyst ink slurries were prepared with water, isopropanol, propanediol and Nafion solutions added to catalyst powders. The slurry was homogenized with Hielsher 400S ultrasonic homogenizer at full power (400 W) with intermittent cycles. Excess isopropanol, which was used for catalyst surface wetting and increased volume for initial homogenization, was removed slowly by evaporation in air.

The catalyst slurry was coated on 125 μm thick Teflon sheets through a 120 mesh silk screen masked for 5 cm^2 coatings. A Pt loading of 0.3 mg Pt cm^{-2} and 25 wt% Nafion concentration were selected for all coatings. Nafion 212 (50 μm) was placed between two catalysts layers between Teflon sheets. The sandwich then was

Table 1
TGA, BET and DLS results.

Material	TGA (wt%)			BET surface area ($m^2 g^{-1}$)	DLS particle Size (nm)
	C %	SiO_2 %	Pt %		
CS1	100	0	0	320.8	300.54
CS2	95.51	4.49	0	212.5	193.7
CS3	89.12	10.88	0	383.3	258.7
CS4	84.66	16.34	0	523.0	259.1
Aerogel silica	–	–	–	751[a]	44.86[b]
Cat1	55.15	0	44.85	193.2	–
Cat2	52.97	2.38	44.65	164.4	–
Cat3	56.54	6.16	37.30	396.3	–
Cat4	50.57	8.24	41.19	337.2	–

[a] BET surface area of aerogel silica was reported by Van Bommel et al. [59].
[b] DLS analysis was carried out after 96 h stirring.

hot pressed under 150 N cm^{-2} pressure at 130 °C for 8 min. The coatings became adherent to Nafion during heating creating membrane electrode assemblies (MEAs) that were subsequently peeled from the Teflon sheets [51].

2.6. Fuel cell performance tests

As-prepared MEAs were tested using a Scribner 850C fuel cell test station and a 5 cm^2 test cell. MEAs were placed between two 0.5 mm thick gas diffusion layers (GDLs) (ELAT GDL/LP/NC/V3.1) and two 0.2 mm thick silicone gaskets. Performance tests were conducted at 60 °C with 100% humidified H_2 (0.2 l min^{-1}) and O_2 (0.5 l min^{-1}). Backpressure (2 atm) was generated on both sides with relief valves. A 140 N cm^{-2} homogeneous clamping pressure was obtained with a torque wrench. MEAs were conditioned with slow increments in current withdrawal at 60 °C before recording a performance test.

Active MEA surface areas were determined after the performance test by purging with 100% humidified N_2 instead of O_2 on the cathode side. The potential was swept between 0 and 1 V with 20 mV s^{-1} scan rate. 0.5 l min^{-1} H_2 and N_2 flow rates were kept constant during the analysis.

2.7. Fuel cell durability tests

Sustainability of the MEA performances were evaluated with accelerated durability tests. There are several accelerated durability tests for catalyst durability evaluation [52–59]. Among these, potential cycling between 0.6 and 1.2 V for 1 day was selected resulting in 1440 cycles at 20 mV s^{-1} scan rate [59]. Decreases in active surface area and fuel cell performance at certain potentials were recorded.

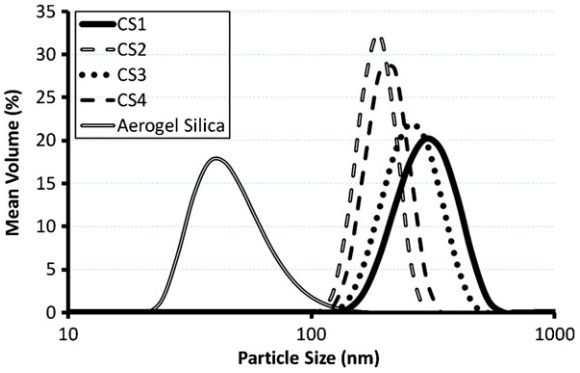

Fig. 1. Particle size distribution of support materials.

3. Results and discussion

3.1. Physical properties of support materials and catalysts

Three carbon–silica composite materials (5, 10, 15 wt% SiO_x) were prepared to investigate the effect of siliceous component addition on Vulcan XC-72. Subsequently, four different catalysts were synthesized with these support materials that included a silica-free control. TGA in air was used to estimate C-SiO_2 concentrations of supports and catalysts [48]. Carbon is removed by combustion in air. The mass concentration of remaining components were calculated by difference. TGA analysis results of the prepared support materials and catalysts are summarized in Table 1.

Surface areas of the prepared support materials and catalysts were determined with BET surface area analysis [50]. Surface area

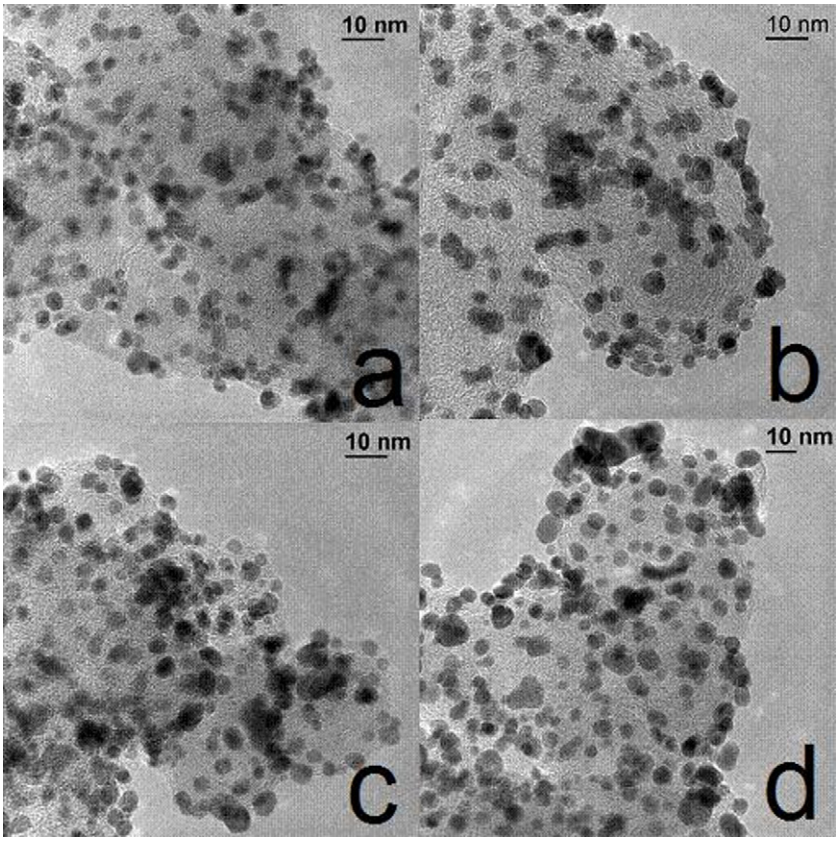

Fig. 2. TEM images of synthesized catalysts (a) Cat1, (b) Cat2, (c) Cat3, and (d) Cat4.

Table 2
Active surface area change during the durability test.

MEA	Support material	Catalyst	% SiO_2 (wt%)	Initial active surface area (m^2/g_{Pt})	Final active surface area (m^2/g_{Pt})	Active surface area loss (%)
MEA1	CS1	Cat1	0	27.88	17.81	36.1
MEA2	CS2	Cat2	2.49	15.20	10.66	29.9
MEA3	CS3	Cat3	6.90	13.92	10.51	24.5
MEA4	CS4	Cat4	9.76	14.92	11.98	19.7

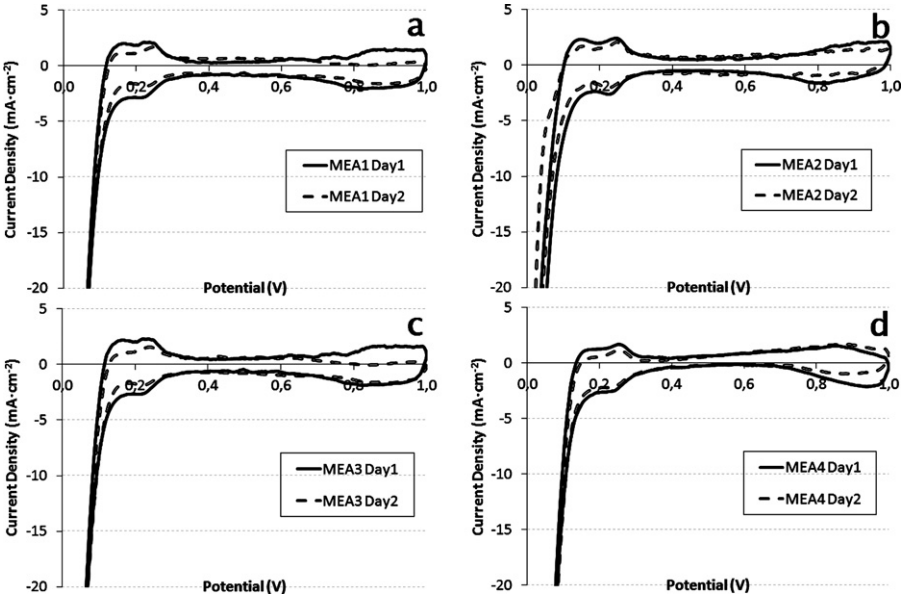

Fig. 3. Active surface area change after 1 day durability test (a) Cat1, (b) Cat2, (c) Cat3, and (d) Cat4.

change with silica addition is summarized in Table 1. The results indicate that the silica deposition increased the surface area of the support materials after certain concentrations. This rise was expected, since BET surface area of solid aerogel silica was reported to be 751 $m^2\,g^{-1}$ [60]. Similar results were obtained with catalysts, although the increase in surface area was not regular, with Cat2 < Cat3 but Cat3 > Cat4.

Particle size of support materials and silica were determined with DLS analysis. Spherical sub micron sized Vulcan XC-72 particles have tendency to agglomeration. The results summarized in Table 1 Indicate particle size of C-SiO_2 composite support materials is smaller than Vulcan XC-72 (CS1). No peak was observed at 40 nm (Fig. 1), which confirmed that aerogel silica was not discrete in the structure. Decreased particle size may be due to Vulcan XC-72 agglomerates being disrupted by ultrasonic agitation that coupled with stabilization from aerogel silica. This observation is related to the finding of Morris, et al. who used the term "nanoglue".

$NaBH_4$ reduction method was used for catalyst synthesis [49]. Platinum particle size was determined by TEM. The results indicated 2–5 nm platinum particle size formation for all catalysts. Homogeneous platinum distribution on carbon was obtained with all catalysts as shown in Fig. 2. Pt agglomeration was somewhat more pronounced with high SiO_2 containing catalysts (Cat 3 and 4). Presence of residual SiO_x groups increases the adsorption sites for platinum locally which might have favored platinum agglomeration around those local points. Additionally, slow removal of water from the support material surface might enable dissolution and precipitation mechanism to continue at very slow rates. Furthermore, secondary Van der Waals forces might result in bridging between Si and Pt atoms as Si–O–Pt, which might cause existence of larger platinum particles. As expected, platinum agglomeration increased with increasing SiO_x content.

3.2. Fuel cell performance and durability experiments

A standard MEA preparation method, screen printing acoupled with decal transfer, was followed for all catalysts. Active surface area measurements were conducted to obtain the pure kinetic activity of the catalysts theoretically so as to compare with results of performance and durability experiments.

3.3. Active surface area measurements

Active surface area measurements were conducted on cathode sides of the MEAs. The results were used to determine catalyst layer activity. Durability of the catalysts was also examined with active surface area change during the durability test. Active surface areas of the MEAs prepared with different support materials before and

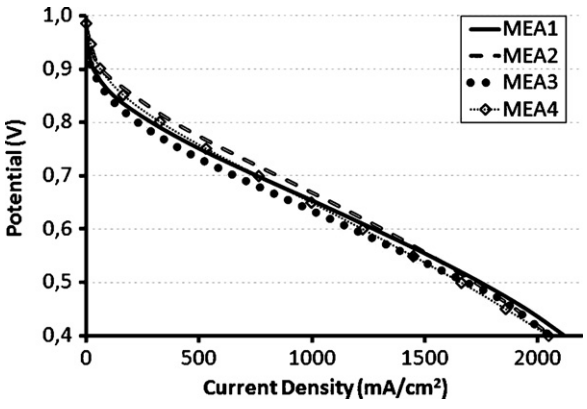

Fig. 4. Fuel cell performance comparison of prepared MEAs.

Table 3
Fuel cell performance loss of prepared MEAs.

MEA	Support Material	Catalyst	% SiO_2 (wt%)	Initial current density @ 0.6 V (mA cm^{-2})	Final current density @ 0.6 V (mA cm^{-2})	Performance loss (%)
MEA1	CS1	Cat1	0	881	531	39.7
MEA2	CS2	Cat2	2.49	825	499	39.5
MEA3	CS3	Cat3	6.90	972	740	23.9
MEA4	CS4	Cat4	9.76	788	614	22.1

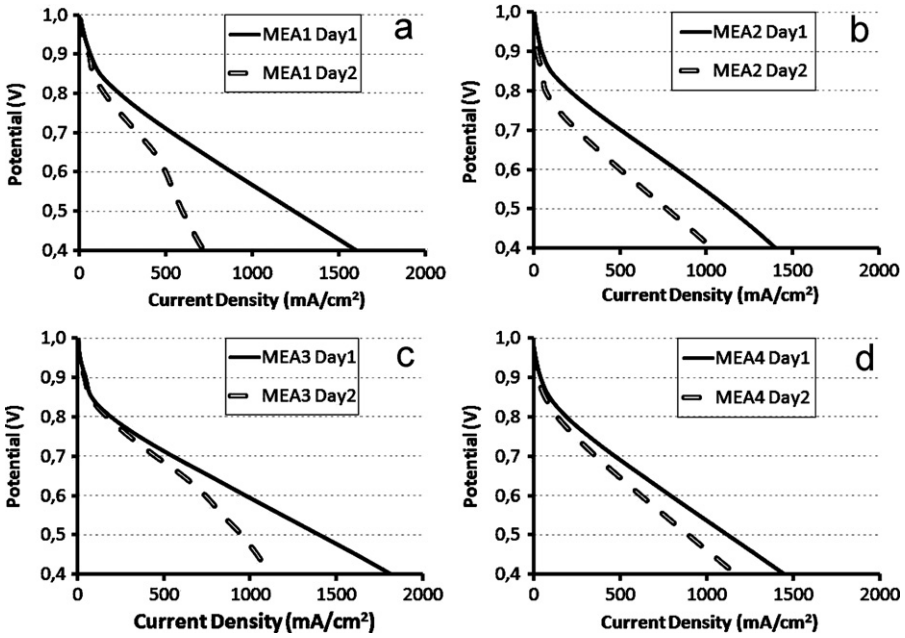

Fig. 5. Performance loss after 1 day accelerated durability test (a) Cat1, (b) Cat2, (c) Cat3, and (d) Cat4.

after the durability test is summarized in Table 2 and shown in Fig. 3. The results indicate that active surface area of all catalysts dropped after the 1 day durability test. In addition to this, the double capacity layer indicating the surface charge capacity of the catalysts had increased after the test. Increase in double capacity layer thickness was limited with increasing silica content. The results for high silica containing Cat 3 and Cat 4 showed that the double capacity layer thickness had hardly changed, which might indicate protection of the morphology.

3.4. Performance results

Fuel cell performances was compared by matching polarization curves obtained at 60 °C. The polarization curve comparison of prepared MEAs is shown in Fig. 4.

The results indicate that silica modification up to 2.5 wt% slightly increased the performance. This increase might be related to better access to platinum by an improved mesoporous structure, since aerogel silica network consists mostly of meso (43 vol%) and macro (49 vol%) pores [60]. Micropores of Vulcan XC-72 might be blocked by addition of siliceous components at low levels. However, further increase in silica amount decreased the performance, which might be attributed to a drop in electrical conductivity of the catalyst layer. On the other hand, mass transport losses became more apparent at high current values for silica containing MEAs. Perhaps this is due to increased hydrophilic character due to siliceous modification.

3.5. Durability results

Durability of the MEAs were also examined with accelerated durability experiments. Performance decreases in polarization curves for all four catalysts are shown in Fig. 5. Current density drop at 0.6 V was selected to quantify the performance loss (Table 3).

In general, MEA durability was improved with increasing silica content. MEAs prepared with 6.0 wt% silica containing catalysts showed highest performance after the 1 day durability test. Electrochemical reactions at both anode and cathode sides of fuel cell require effective electron transfer process. The silica in the structure might have slowed down the electron transfer process, which had slightly decreased the performance but also slowed down the electron transfer required for corrosion reactions.

These new composite materials are very promising materials especially for low humidity applications. Furthermore, hydrophillic behavior of silica particles might be helpful for internal humidification of the catalyst layer. Varying power needs of fuel cell systems lead to excess water generation and dry operating conditions, frequently. Condensed water on silica which occurs at high power applications might improve the ionic conductivity in the catalyst layer for low power applications.

4. Conclusion

Carbon-aerogel silica composite structures were prepared as an alternative catalyst support material for PEM fuel cells. Platinum

catalysts were prepared using several C-SiO_2 composite support materials with various SiO_2 concentrations. Material characteristics of support materials and catalysts were determined. MEAs were prepared with synthesized catalysts and tested to investigate the effect of novel support material on fuel cell performance and durability. In general the results showed that C-aerogel SiO_2 composites are promising candidates as a durable support material. Performance of the MEAs with limited SiO_2 content was improved compared to silica-free MEAs, probably due to homogeneous carbon distribution. However, MEAs with high SiO_2 content showed lower but acceptable performance limited by the insulating behavior of silica. On the other hand, mass transport losses increased with hydrophilic nature of silica. This fact limits their use at high current density. However, this might be useful for circumstances requiring internal humidification. In conclusion, novel carbon-aerogel silica composite materials are good candidates as a catalyst support material for durable high performance MEAs.

Acknowledgement

Support from the NASA Space Science Office (Grant Number NNC04GB13G) is gratefully acknowledged.

References

[1] F.A. de Bruijn, V.A.T. Dam, G.J.M. Janssen, Fuel Cells 8 (2008) 3–22.
[2] C.D. Huang, K.S. Tan, H.Y. Lin, K.L. Tan, Chem. Phys. Lett. 371 (2003) 80–85.
[3] C. Iojoiu, E. Guilminot, F. Maillard, M. Chatenet, J.Y. Sanchez, E. Claude, E. Rossinot, J. Electrochem. Soc. 154 (2007) B1115–B1120.
[4] M. Cappadonia, J.W. Erning, U. Stimming, J. Electroanal. Chem. 376 (1994) 189–193.
[5] M. Cappadonia, J.W. Erning, S.M.S. Niaki, U. Stimming, Solid State Ionics 77 (1995) 65–69.
[6] Y.S. Kim, L.M. Dong, M.A. Hickner, T.E. Glass, V. Webb, J.E. McGrath, Macromolecules 36 (2003) 6281–6285.
[7] M. Saito, K. Hayamizu, T. Okada, J. Phys. Chem. B 109 (2005) 3112–3119.
[8] R.C. McDonald, C.K. Mittelsteadt, E.L. Thompson, Fuel Cells 4 (2004) 208–213.
[9] R. Borup, J. Meyers, B. Pivovar, Y.S. Kim, R. Mukundan, N. Garland, D. Myers, M. Wilson, F. Garzon, D. Wood, P. Zelenay, K. More, K. Stroh, T. Zawodzinski, J. Boncella, J.E. McGrath, M. Inaba, K. Miyatake, M. Hori, K. Ota, Z. Ogumi, S. Miyata, A. Nishikata, Z. Siroma, Y. Uchimoto, K. Yasuda, K.-i. Kimijima, N. Iwashita, Chem. Rev. 107 (2007) 3904–3951.
[10] D.L. Wood, R.L. Borup, Durability aspects of gas-diffusion and microporous layers, in: F.N. Büchi, M. Inaba, T.J. Schmidt (Eds.), Polymer Electrolyte Fuel Cell Durability, Springer Science + Business Media LLC, 2009, pp. 159–195.
[11] O.L. Adrianowycz, Next Generation Bipolar Plates for Automotive PEM Fuel Cells, GrafTech International Ltd, 2009, pp. 1108–1112.
[12] J. Scherer, D. Münter, R. Ströbel, Influence of metalic bipolar plates on the durability of polymer electrolyte fuel cells, in: F.N. Büchi, M. Inaba, T.J. Schmidt (Eds.), Polymer Electrolyte Fuel Cell Durability, Springer Science + Business Media LLC, 2009, pp. 243–255.
[13] M. Schulze, T. Knori, A. Schneider, E. Gulzow, J. Power Sources 127 (2004) 222–229.
[14] J.Z. Tan, Y.J. Chao, J.W. Van Zee, W.K. Lee, Mater. Sci. Eng. A: Struct. 445 (2007) 669–675.
[15] M.A. Travassos, C.M. Rangel, Hydrogen Energy and Sustainability—Advances in Fuel Cells and Hydrogen Workshop, Torres Vedras, Portugal, 2010, pp. 48–52.
[16] J. Sinha, S. Lasher, Y. Yang, DOE Annual Merit Review, Arlington, VA, USA, 2009.
[17] S. Zhang, X.-Z. Yuan, J.N.C. Hin, H. Wang, K.A. Friedrich, M. Schulze, J. Power Sources 194 (2009) 588–600.
[18] F.N. Büchi, Heteregenous cell ageing in polymer electrolyte fuel cell stacks, in: F.N. Büchi, M. Itaba, T.J. Schmidt (Eds.), Polymer Electrolyte Fuel Cell Durability, Springer Science Business Media LLC, 2009, pp. 431–439.
[19] W.A. Adams, J. Blair, K.R. Bullock, C.L. Gardner, J. Power Sources 145 (2005) 55–61.
[20] M.V. Lauritzen, P. He, A.P. Young, S. Knights, V. Colbow, P. Beattie, J. New Mater. Electrochem. Syst. 10 (2007) 143–145.
[21] X. Wang, W.Z. Li, Z.W. Chen, M. Waje, Y.S. Yan, J. Power Sources 158 (2006) 154–159.
[22] C.H. Yen, K. Shimizu, Y.-Y. Lin, F. Bailey, I.F. Cheng, C.M. Wai, Energy Fuels 21 (2007) 2268–2271.
[23] Y.Y. Shao, G.P. Yin, Y.Z. Gao, J. Power Sources 171 (2007) 558–566.
[24] K. Lee, J. Zhang, H. Wang, D.P. Wilkinson, J. Appl. Electrochem. 36 (2006) 507–522.
[25] W. Bi, T.F. Fuller, ECS Trans. 11 (2007) 1235–1246.
[26] S. Guo, S. Dong, E. Wang, J. Phys. Chem. C 112 (2008) 2389–2393.
[27] G.R. Dieckmann, S.H. Langer, Electrochim. Acta 44 (1998) 437–444.
[28] G. Wu, L. Li, J.H. Li, B.Q. Xu, Carbon 43 (2005) 2579–2587.
[29] Z. Lei, S. Bai, Y. Xiao, L. Dang, L. An, G. Zhang, Q. Xu, J. Phys. Chem. C 112 (2008) 722–731.
[30] E.P. Ambrosio, C. Francia, C. Gerbaldi, N. Penazzi, P. Spinelli, M. Manzoli, G. Ghiotti, J. Appl. Electrochem. 38 (2008) 1019–1027.
[31] M. Sevilla, C. Sanchis, T. Valdes-Solis, E. Morallon, A.B. Fuertes, Carbon 46 (2008) 931–939.
[32] X. Luo, Z. Hou, P. Ming, Z. Shao, B. Yi, Cuihua Xuebao 29 (2008) 330–334.
[33] W. Bi, T.F. Fuller, J. Electrochem. Soc. 155 (2008) B215–B221.
[34] S.C. Mu, H.F. Lv, N.C. Cheng, M. Pan, Appl. Catal. B: Environ. 100 (2010) 190–196.
[35] J. Yi, J.B. Joo, J. Kim, P. Kim, J. Nanosci. Nanotechnol. 10 (2010) 3397–3401.
[36] S. Dai, Q. Zhu, S.H. Zhou, X.Q. Wang, J. Power Sources 193 (2009) 495–500.
[37] A. Bonakdarpour, J. Wenzel, D.A. Stevens, S. Sheng, T.L. Monchesky, R. Lobel, R.T. Atanasoski, A.K. Schmoeckel, G.D. Vernstrom, M.K. Debe, J.R. Dahn, J. Electrochem. Soc. 152 (2005) A61–A72.
[38] F. Dundar, A. Smirnova, X. Dong, A. Ata, N. Sammes, J. Fuel Cell Sci. Technol. 3 (2006) 428–433.
[39] C.J. Brinker, G.W. Scherer, Sol–gel Science: The Physics and Chemistry of Sol–gel Processing, Academic Press, 1990.
[40] M.L. Anderson, R.M. Stroud, D.R. Rolison, Nano Lett. 2 (2002) 235–240.
[41] J. Wang, J. Kuhn, X. Lu, J. Non-Cryst. Solids 186 (1995) 296–300.
[42] C. Lorenz, A. Emmerling, J. Fricke, T. Schmidt, M. Hilgendorff, L. Spanhel, G. Muller, J. Non-Cryst. Solids 238 (1998) 1–5.
[43] C. Rutiser, S. Komarneni, R. Roy, Mater. Lett. 19 (1994) 221–224.
[44] S. Dire, F. Babonneau, G. Carturan, J. Livage, J. Non-Cryst. Solids 147 (1992) 62–66.
[45] K. Fujiki, T. Ogasawara, N. Tsubokawa, J. Mater. Sci. 33 (1998) 1871–1879.
[46] C.A. Morris, M.L. Anderson, R.M. Stroud, C.I. Merzbacher, D.R. Rolison, Science 284 (1999) 622–624.
[47] S. Takenaka, H. Matsumori, T. Arike, H. Matsune, M. Kishida, Top. Catal. 52 (2009) 731–738.
[48] O.A. Pinchuk, F. Dundar, A. Ata, K.J. Wynne, Int. J. Hydrogen Energy, doi:10.1016/j.ijhydene.2011.10.093, corrected proof, in press.
[49] K.W. Park, J.H. Choi, S.A. Lee, C. Pak, H. Chang, Y.E. Sung, J. Catal. 224 (2004) 236–242.
[50] S. Brunauer, P.H. Emmett, E. Teller, J. Am. Chem. Soc. 60 (1938) 309–319.
[51] N. Rajalakshmi, K.S. Dhathathreyan, Chem. Eng. J. 129 (2007) 31–40.
[52] K. More, in: V. Lightner (Ed.), Microstructural Characterization Of PEM Fuel Cell MEAs, Oak Ridge National Lab (ORNL), Arlington, VA, USA, 2005.
[53] J. Frisk, W. Boand, M. Hicks, M. Kurkowski, R. Atanasoski, A. Schmoeckel, Fuel Cell Seminar, Courtesy Associates, San Antonio, TX, USA, 2004.
[54] R.L. Borup, J.R. Davey, F.H. Garzon, D.L. Wood, M.A. Inbody, J. Power Sources 163 (2006) 76–81.
[55] Y.Y. Shao, G.P. Yin, J.J. Wang, Y.Z. Gao, P.F. Shi, J. Electrochem. Soc. 153 (2006) A1261–A1265.
[56] T. Rockward, F. Uribe, in: V. Lightner (Ed.), Component Benchmarking: Establishing a Standardized Single Cell Testing Procedure through Industry Participation, Consensus and Experimentation, Los Alamos National Laboratory, 2005, pp. 1052–1055.
[57] L.M. Roen, C.H. Paik, T.D. Jarvic, Electrochem. Solid-State Lett. 7 (2004) A19–A22.
[58] DOE, Available online at http://www1.eere.energy.gov/hydrogenandfuelcells/fuelcells/pdfs/component_durability_profile.pdf, last acccessed on 23.12.2011, 2007.
[59] Y.G. Chen, J.J. Wang, H. Liu, R.Y. Li, X.L. Sun, S.Y. Ye, S. Knights, Electrochem. Commun. 11 (2009) 2071–2076.
[60] M.J. Van Bommel, C.W.d. Engelsen, J.C. Van Miltenburg, J. Porous Mater. 4 (1997) 143–150.